# Continuum treatment of phonon polaritons in semiconductor heterogeneous structures

F. Comas
*Department of Theoretical Physics, Havana University, Vedado 10400, Havana, Cuba*

C. Trallero-Giner* and M. Cardona
*Max-Planck-Institut für Festkörperforschung, Heisenbergstrasse 1, 70569 Stuttgart, Federal Republic of Germany*
(Received 16 August 1996)

A phenomenological approach is applied to the theory of phonon polaritons in semiconductor heterogeneous structures, with special emphasis on semiconductor nanostructures. Applying the macroscopic approach to continuous media, seven coupled partial differential equations are derived for the fundamental quantities involved: the three components of the displacement field **u**, those of the magnetic potential **A**, and the electric potential $\phi$ in the Lorentz gauge. Our treatment is rather general in its conception: no assumptions on the system geometry and composition are made. We develop a general method allowing us to obtain the exact analytical solutions of the equations when the constituent materials can be assumed to be isotropic. The matching boundary conditions at the structure interfaces are derived from the differential equations and interpreted in physical terms. This theory leads to a phenomenological description of phonon polaritons valid in the long-wavelength limit. We apply it to the case of the double heterostructure, and calculate both the mechanical displacements **u** and the potentials **A**, $\phi$ of normal modes in the GaAs/AlAs prototype system. We also discuss the dispersion relations for these modes which are of transverse-electric and transverse-magnetic character. A comparison is made with some limiting cases: the unretarded case ($c \rightarrow \infty$) reproducing our previous results for polar-optical phonons, and the nondispersive case ($\beta_T \rightarrow 0$), which leads to the Fuchs-Kliewer slab modes. [S0163-1829(97)03731-4]

## I. INTRODUCTION

The long-wavelength optical vibrations of semiconductor nanostructures have been the subject of extensive studies in the past years.[1] However, since the early papers of Kliewer-Fuchs[2,3] and Ruppin-Englman,[4] only a few works[5–8] have been devoted to the investigation of phonon-polariton modes in such systems as quantum wells, superlattices, quantum wires, etc. Raman scattering by interface-phonon polaritons in an Air/GaAs/AlAs structure was reported in Ref. 9 and the dispersion relation for polariton modes evaluated along the lines of the dielectric model in quantum-well superlattices[10–12] and quantum-wire superlattices[13] have been also discussed. The theory of phonon polaritons in low-dimensional semiconductor structures requires reconsideration with respect to that of bulk semiconductors. The mesoscopic dimensions of the system, the presence of interfaces, as well as details of the geometry and fabrication lead to fundamental changes in the physical situation. Thus, a new theoretical treatment is needed.

For the long-wave limit we consider a phenomenological macroscopic approach. In the phenomenological treatment of polar-optical phonons in semiconductor nanostructures this kind of approach has provided rather satisfactory results (see Refs. 14–16 and references therein). Polar-optical phonons should be contained in the phonon polaritons as a limit when retardation effects in the electromagnetic field are neglected ($c \rightarrow \infty$). We thus expect that phonon polaritons should also be well described with a phenomenological approach. The existing literature on the subject suggests that a general consistent discussion in the case of semiconductor nanostructures, making a systematic application of the physics of continuous media, is lacking. Such a discussion is the aim of the present work.

Here we present a general theoretical discussion of phonon polaritons for nanostructures of arbitrary shape and structure. We start from a Lagrangian density considering a mechanical displacement field **u** and the electromagnetic field described by the potentials **A** and $\phi$ in the Lorentz gauge. The medium is characterized by its elastic and dielectric properties, but assumed to be nonmagnetic and, in the most general case, the anisotropy of the constituent materials is considered. The material physical properties experience abrupt steplike changes at the interfaces, which are then treated by means of appropriate matching-boundary conditions which are derived directly from the differential equations and interpreted in physical terms. We are thus led to seven coupled second-order partial differential equations. Their solution yields the normal modes which, in our case, bear a dispersive character. These modes are neither purely transverse nor longitudinal, but of a mixed nature, in close analogy with the results obtained in the case of polar-optical phonons.[17,18] The purpose of this work is the development of a general mathematical method allowing us to generate the analytical solutions of the coupled differential equations when each homogeneous part of the structure is assumed isotropic in its elastic and electromagnetic properties. The method is rather general and can be applied to nanostructures of different geometry and composition. As an example the method is applied to a double heterostructure (DHS) with matching-boundary conditions suitable for the GaAs/AlAs prototype. For this kind of system a high confinement of the mechanical vibrations is expected within each layer. We explicitly calculate analytical expressions for **u**, **A**, and $\phi$ giving a detailed discussion of the TE and TM oscillation modes and the corresponding dispersion relations.

## II. THEORETICAL ANALYSIS OF THE MODEL

Let us consider polar semiconductor compounds of the zinc-blende type. The field $\mathbf{u}(\mathbf{r},t)$ (with units of length) represents the relative displacement of the ions from their equilibrium positions. The vector $\mathbf{u}$ is treated in the spirit of the theory of continuous media. Coupled to the displacement vector there is an electromagnetic field with the electric- and magnetic-field intensities $\mathbf{E}(\mathbf{r},t)$ and $\mathbf{H}(\mathbf{r},t)$. They are related to the electromagnetic potentials $\mathbf{A}(\mathbf{r},t)$ and $\phi(\mathbf{r},t)$ by

$$\mathbf{E}=-\nabla\phi-\frac{1}{c}\frac{\partial\mathbf{A}}{\partial t};\quad \mathbf{H}=\boldsymbol{\nabla}\times\mathbf{A}, \tag{1}$$

which satisfy the Lorentz gauge:

$$\boldsymbol{\nabla}\cdot\mathbf{A}+\frac{1}{c}\frac{\partial\phi}{\partial t}=0. \tag{2}$$

For a given homogeneous segment of the system we introduce the following Lagrangian density:

$$\mathcal{L}=\frac{1}{2}\rho\frac{\partial u_j}{\partial t}\frac{\partial u_j}{\partial t}+\frac{1}{2}\gamma_{jl}u_ju_l+\frac{1}{2}\lambda_{jlmn}\frac{\partial u_j}{\partial x_l}\frac{\partial u_m}{\partial x_n}+\frac{1}{8\pi}\beta_{jl}E_jE_l-\alpha_{jl}u_jE_l+\frac{1}{8\pi}H_jH_j. \tag{3}$$

In all the equations the subscripts take values 1, 2, and 3 labeling the Cartesian components of vectors and tensors. Moreover, the summation convention over repeated indices is assumed (unless the contrary is stated). $\rho$ is the reduced-mass density, $\gamma_{jl}$ a symmetric tensor coupling the mechanical displacement field with itself, $\beta_{jl}$ a symmetric tensor coupling the electric field with itself, and $\alpha_{jl}$ a tensor (not necessarily symmetric) coupling the displacement with the electric field. The fourth rank tensor $\lambda_{jlmn}$ describes elastic properties of the medium.[15,19] Hence, the third term at the right-hand side of Eq. (3) represents internal stresses in the medium and leads to dispersive oscillation modes. Finally, the last term at the right-hand side of Eq. (3) is the energy density of the magnetic field, the same as in a vacuum since we assume a nonmagnetic medium.

We have found it convenient to use $u_j$, $A_j$, and $\phi$ as the generalized coordinates of this system. Equations (1) must then be substituted in Eq. (3) in order to obtain

$$\mathcal{L}=\mathcal{L}\left(u_j,\frac{\partial u_j}{\partial x_l},A_j,\frac{\partial A_j}{\partial x_l},\phi,\frac{\partial\phi}{\partial x_l}\right). \tag{4}$$

All the arguments in $\mathcal{L}$ appear quadratically, thus leading to linear differential equations. The tensor character of the parameters allows us to consider the anisotropy of the constituent materials. Moreover, all parameters are assumed to show steplike abrupt changes at the interfaces of the nanostructure.

Straightforward application of the Lagrange equations leads to the following equations:[20]

$$\rho\frac{\partial^2u_j}{\partial t^2}=\gamma_{jl}u_l-\frac{\partial}{\partial x_l}\sigma_{jl}+\alpha_{jl}E_l; \tag{5}$$

$$(\boldsymbol{\nabla}\times\mathbf{H})_j=\frac{1}{c}\frac{\partial}{\partial t}D_j; \tag{6}$$

$$\frac{\partial}{\partial x_l}D_l=0, \tag{7}$$

where

$$D_j=\beta_{jl}E_l+4\pi\alpha_{jl}u_l. \tag{8}$$

Equations (5)–(7) could have been written directly by inspection as a generalization of those given in Ref. 17 so as to add electromagnetic propagation effects (retardation). Here, however, we have used the Lagrangian formulation which is crucial if one wants to quantize the fields involved.[18]

In the equations above we have introduced the effective ''stress'' tensor:

$$\sigma_{jl}=\lambda_{jlmn}\frac{\partial u_m}{\partial x_n}; \tag{9}$$

applying the same notation as in Ref. 19. Using the expression $\mathbf{D}=\mathbf{E}+4\pi\mathbf{P}$ the material relation can also be written as

$$P_j=\frac{1}{4\pi}(\beta_{jl}-\delta_{jl})E_l+\alpha_{jl}u_l, \tag{10}$$

where $\delta_{jl}$ is the Kronecker $\delta$. The remaining Maxwell equations are directly derived from Eq. (1) and read

$$\boldsymbol{\nabla}\cdot\mathbf{H}=0,\quad \boldsymbol{\nabla}\times\mathbf{E}=-\frac{1}{c}\frac{\partial\mathbf{H}}{\partial t}. \tag{11}$$

For the sake of compactness and ease of their physical interpretation we have written the above equations in terms of vector fields $\mathbf{E}$, $\mathbf{H}$, and $\mathbf{D}$ instead of the potentials $\mathbf{A}$ and $\phi$. As stressed before, these equations are valid within each homogeneous portion of the structure. Let us assume:

$$\mathbf{u}(\mathbf{r},t)=\mathbf{u}(\mathbf{r})e^{-i\omega t},\quad \mathbf{A}(\mathbf{r},t)=\mathbf{A}(\mathbf{r})e^{-i\omega t},$$
$$\text{and}\ \ \phi(\mathbf{r},t)=\phi(\mathbf{r})e^{-i\omega t}.$$

The physical parameters entering our equations should be given in terms of macroscopic physical properties of the medium by the straightforward application of well-known procedures.[21] We thus have the following results:

$$\gamma_{jl}=-\rho\omega_{0j}^2\delta_{jl}\quad \text{(without summation convention)}; \tag{12}$$

where $\omega_{0j}$ are the characteristic oscillation frequencies of the medium (TO phonons at $k\simeq0$) along the fundamental symmetry directions. We also have

$$\beta_{jl}=\epsilon_{jl}^{\infty}. \tag{13}$$

The tensor $\alpha_{jl}$ must be determined by solving the system of algebraic equations:

$$\alpha_{il}\gamma_{kl}^{-1}\alpha_{kj}=\frac{1}{4\pi}[\epsilon_{ij}^{0}-\epsilon_{ij}^{\infty}]. \tag{14}$$

In the above equations $\epsilon_{jl}^{\infty}(\epsilon_{jl}^{0})$ is the high-frequency (static) dielectric constant tensor of the medium.

Using Eqs. (12)–(14), Eqs. (5), (6), and (7) can be transformed into

$$\rho(\omega^2-\omega_{0j}^2)u_j=\frac{\partial}{\partial x_l}\,\sigma_{jl}-\frac{i\omega}{c}\,\alpha_{jl}A_l+\alpha_{jl}\,\frac{\partial\phi}{\partial x_l}; \quad (15)$$

$$\nabla^2A_j+\frac{\omega^2}{c^2}\,\epsilon_{jl}^{\infty}A_l=-\frac{i\omega}{c}\left[(\epsilon_{jl}^{\infty}-\delta_{jl})\,\frac{\partial\phi}{\partial x_l}-4\pi\alpha_{jl}u_l\right]; \quad (16)$$

$$\epsilon_{jl}^{\infty}\,\frac{\partial^2\phi}{\partial x_j\partial x_l}=\frac{i\omega}{c}\,\epsilon_{jl}^{\infty}\,\frac{\partial A_j}{\partial x_l}+4\pi\alpha_{jl}\,\frac{\partial u_j}{\partial x_l}. \quad (17)$$

This is a system of seven second-order coupled partial differential equations. However, it is important to note that only six of these equations are linearly independent. In fact Eq. (17) follows from Eq. (16) when the Lorentz condition [Eq. (2)] is applied. In all the subsequent equations the fundamental quantities describing the fields are explicit functions of only $\mathbf{r}$. In principle, the solutions of the above equations can be written in the form of certain ''six-vectors'' $\mathbf{F}=[\mathbf{u},\mathbf{A}]$, a notation which will prove to be very useful. In order to span the solution space in each homogeneous region we must determine twelve six-vectors $\mathbf{F}_n$ representing a given basis for the solution space, while the general solution will be a linear combination of these six-vectors. The admixture coefficients must, of course, be determined by imposing the matching boundary conditions at each interface.

### A. Matching boundary conditions

As in Ref. 17, the matching boundary conditions must be derived from the fundamental equations of our model, i.e., Eqs. (15)–(17) and (11) and should have a transparent physical meaning. In the first place we must require the functions $\mathbf{u}$, $\mathbf{A}$, and $\phi$ to be bounded and continuous in the whole space. Moreover, the standard boundary conditions of classical electrodynamics should be fulfilled. Hence, according to Eqs. (6), (7), and (11), the following quantities must be continuous at each interface of the structure: (i) $D_N=\mathbf{D}\cdot\mathbf{N}$; (ii) $H_N=\mathbf{H}\cdot\mathbf{N}$; (iii) $H_T=\mathbf{H}\cdot\mathbf{T}$; (iv) $E_T=\mathbf{E}\cdot\mathbf{T}$. In the expressions above the vector $\mathbf{N}(\mathbf{T})$ is the unit vector normal (tangential) to the interface surface.

Another important matching boundary condition is derived from Eq. (15) and is thus related to the mechanical aspects of the problem. By fairly standard techniques (see for instance Ref. 17) we are led to the continuity of (v) $\boldsymbol{\sigma}_N=\boldsymbol{\sigma}\cdot\mathbf{N}$, at each interface of the structure.

The above conditions applied at all interfaces between homogeneous parts of the system completely determine the solutions of the mathematical problem. From a rigorous analysis of the fundamental equations we have to require the continuity: $\mathbf{u}$, $\mathbf{A}$, $\phi$, $\boldsymbol{\sigma}_N$, $D_N$, and $H_T$ (twelve conditions for the twelve constants present in the general solutions). The remaining quantities involved ($H_N$ and $E_T$) are then automatically continuous at the interfaces.

### B. Solution method

We present next a method for generating analytical solutions of the Eqs. (15)–(17) irrespective of the particular geometry and nature of the nanostructure under consideration. We shall limit ourselves to the case where the constituent materials are modeled as isotropic continuous media. For such a case Eqs. (15)–(17) read

$$\Lambda_1\nabla^2\mathbf{u}+\Lambda_2\nabla\nabla\cdot\mathbf{u}-\rho(\omega^2-\omega_0^2)\mathbf{u}=\frac{i\omega}{c}\,\alpha\mathbf{A}-\alpha\nabla\phi; \quad (18)$$

$$\nabla^2\mathbf{A}+\epsilon_\infty\,\frac{\omega^2}{c^2}\,\mathbf{A}=-\frac{i\omega}{c}\,[(\epsilon_\infty-1)\nabla\phi-4\pi\alpha\mathbf{u}]; \quad (19)$$

$$\nabla^2\phi+\frac{\omega^2}{c^2}\,\phi=4\pi\alpha\,\frac{1}{\epsilon_\infty}\,\nabla\cdot\mathbf{u}, \quad (20)$$

where

$$\alpha^2=\frac{1}{4\pi}\,(\epsilon_0-\epsilon_\infty)\rho\omega_0^2, \quad (21)$$

and $\Lambda_1$ and $\Lambda_2$ are two independent phenomenological parameters describing the ''elastic tensor'' $\lambda_{jlmn}$ for an isotropic material. Notice that this tensor is obtained from the curvature of the phonon dispersion relation near $\mathbf{k}=\mathbf{0}$.[14,16,17] The above equations can be solved in the following way. Taking the divergence of Eq. (18), after Eq. (20) is appropriately rewritten we are led to

$$\left[\nabla^2+\frac{1}{\beta_L^2}\,(\omega_L^2-\omega^2)\right]\Psi=0, \quad (22)$$

$$\left[\nabla^2+\frac{\omega^2}{c^2}\right]\phi=\frac{4\pi\alpha}{\epsilon_\infty}\,\Psi, \quad (23)$$

where $\beta_L^2=(\Lambda_1+\Lambda_2)/\rho$, $\Psi=\nabla\cdot\mathbf{u}$, and $\omega_L^2=(\epsilon_0/\epsilon_\infty)\omega_0^2$. Equation (22) is a standard Helmholtz equation with well-known solutions for a given geometry. It is easy to show that the solution of Eq. (23) is

$$\phi=\phi_h+\frac{4\pi\alpha}{\epsilon_\infty}\left[\frac{\omega^2}{c^2}-\frac{1}{\beta_L^2}\,(\omega_L^2-\omega^2)\right]^{-1}\Psi, \quad (24)$$

where $\phi_h$ satisfies the equation

$$\left[\nabla^2+\frac{\omega^2}{c^2}\right]\phi_h=0, \quad (25)$$

which is again a Helmholtz equation. We can thus determine $\Psi$ and $\phi$. Taking the *curl* of Eqs. (18) and (19) we are led to

$$\left[\nabla^2+\frac{1}{\beta_T^2}\,(\omega_0^2-\omega^2)\right]\boldsymbol{\Gamma}=\frac{i\alpha^2}{\rho\beta_T^2}\,\mathbf{S}, \quad (26)$$

$$\left[\nabla^2+\epsilon_\infty\,\frac{\omega^2}{c^2}\right]\mathbf{S}=4\pi i\,\frac{\omega^2}{c^2}\,\boldsymbol{\Gamma}, \quad (27)$$

where

$$\beta_T^2=\Lambda_1/\rho, \quad \boldsymbol{\Gamma}=\nabla\times\mathbf{u}, \quad (28)$$

and we have introduced the dimensionless vector field $\mathbf{S}$ defined by

$$\mathbf{S}=\frac{\omega}{c\alpha}\,\mathbf{H}. \tag{29}$$

The solutions of the set of Eqs. (26) and (27) are of the form:

$$\mathbf{\Gamma}=\mathbf{\Gamma}_h+p_1\mathbf{S} \tag{30}$$

and

$$\mathbf{S}=\mathbf{S}_h+p_2\mathbf{\Gamma}, \tag{31}$$

where $p_i$ $(i=1,2)$ are parameters to be determined below, and $\mathbf{\Gamma}_h$ and $\mathbf{S}_h$ are vectors conveniently chosen to satisfy independent vector Helmholtz equations. Using (30) and (31) it is possible to show that the solutions of Eqs. (26) and (27) are given by

$$\mathbf{\Gamma}=\frac{1}{2}\left(1+\frac{1}{b}\right)\left[\mathbf{\Gamma}_h-\frac{i}{a(1+b)}\,\mathbf{S}_h\right]; \tag{32}$$

$$\mathbf{S}=\frac{1}{2}\left(1+\frac{1}{b}\right)[\mathbf{S}_h+ia(1-b)\mathbf{\Gamma}_h]; \tag{33}$$

with

$$a=\frac{2\pi}{\epsilon_\infty x_0^2}\left(\frac{\omega^2-\omega_0^2x_0^2}{\omega_L^2-\omega_0^2}\right); \tag{34}$$

and

$$b^2=1-4x_0^4\epsilon_\infty(\beta_T/c)^2\,\frac{\omega^2(\omega_L^2-\omega_0^2)}{(\omega^2-\omega_0^2x_0^2)^2}, \tag{35}$$

where the parameter $x_0^2=[1+\epsilon_\infty(\beta_T/c)^2]^{-1}$ has been introduced.

The vector fields $\mathbf{\Gamma}_h$ and $\mathbf{S}_h$ satisfy the Helmholtz equations:

$$(\nabla^2+q^2)\mathbf{\Gamma}_h=0,\quad (\nabla^2+Q^2)\mathbf{S}_h=0; \tag{36}$$

with

$$q^2=\frac{1}{\beta_T^2x_0^2}\left[\frac{1}{2}\,(1-b)(\omega^2-\omega_0^2x_0^2)-x_0^2(\omega^2-\omega_0^2)\right]; \tag{37}$$

$$Q^2=\frac{\epsilon_\infty}{c^2}\left[\frac{1}{2}\,(b-1)\,\frac{\omega^2-\omega_0^2x_0^2}{1-x_0^2}+\omega^2\right]. \tag{38}$$

The methods for solving Eq. (36) are well known and present a simple separated form only in rectangular, cylindric, spherical, elliptical, parabolical, and conical coordinates.[4,22] The particular form of the solutions depends on the geometry of the system. Once the functions $\Psi$, $\phi$, $\mathbf{\Gamma}$, and $\mathbf{S}$ are known, we can determine $\mathbf{u}$ and $\mathbf{A}$. Equation (18) can be rewritten in the form:

$$(\omega^2-\omega_0^2)u=\beta_L^2\nabla\Psi-\beta_T^2\nabla\times\mathbf{\Gamma}-\frac{i\alpha\omega}{\rho c}\,\mathbf{A}+\frac{\alpha}{\rho}\,\nabla_\phi, \tag{39}$$

where the vector identity $\nabla^2\mathbf{u}=\nabla\Psi-\nabla\times\mathbf{\Gamma}$ has been applied. In the same way from the Eq. (19) we obtain:

$$\mathbf{A}=\frac{\alpha c^3}{\epsilon_\infty\omega^3}\,\nabla\times\mathbf{S}-\frac{ic}{\omega}\,\nabla\phi+\frac{4\pi i\alpha c}{\epsilon_\infty\omega}\,\mathbf{u}. \tag{40}$$

Hence, in a rather general way and independently of any particular geometry of the nanostructure, we have shown that the relative mechanical displacement $\mathbf{u}$ and the vector potential $\mathbf{A}$ can be obtained with the following expressions:

$$\mathbf{u}=\frac{1}{\omega^2-\omega_L^2}\left[\beta_L^2\nabla\Psi-\beta_T^2\nabla\times\mathbf{\Gamma}-\frac{ic^2}{4\pi}\,\frac{\omega_L^2-\omega_0^2}{\omega^2}\,\nabla\times\mathbf{S}\right], \tag{41}$$

$$\begin{aligned}\mathbf{A}=&\frac{\alpha c^3}{\epsilon_\infty\omega(\omega^2-\omega_L^2)}\left\{\frac{\omega^2-\omega_0^2}{\omega^2}\,\nabla\times\mathbf{S}-4\pi i(\beta_T/c)^2\nabla\times\mathbf{\Gamma}\right.\\&\left.+4\pi i(\beta_L/c)^4\omega^2\{[1+(\beta_L/c)^2]\omega^2-\omega_L^2\}^{-1}\nabla\Psi\right\}\\&-\frac{ic}{\omega}\,\nabla\phi_h.\end{aligned} \tag{42}$$

These solutions take into account retardation and the coupling between the mechanical displacement field $\mathbf{u}$ and the electromagnetic field described by the potentials $\mathbf{A}$ and $\phi$. We should notice that, as a general property, the vector fields fulfill the conditions: $\nabla\cdot\mathbf{u}\neq 0$, $\nabla\cdot\mathbf{A}\neq 0$ and $\nabla\times\mathbf{u}\neq 0$, $\nabla\times\mathbf{A}\neq 0$, and hence the corresponding modes are neither purely longitudinal nor purely transverse, but bear a mixed character. We must also stress that the influence of $\mathbf{A}$ and $\phi$ on the oscillations does not lead to polariton modes of a purely interface character. The vector field $\mathbf{u}$ in Eq. (41) has three independent contributions: a longitudinal contribution from $\beta_L^2\nabla\Psi$, a transverse contribution proportional to $\beta_T^2\nabla\times\mathbf{\Gamma}$, and a third contribution including the phonon-photon coupling through $(\omega_L^2-\omega_0^2)\nabla\times\mathbf{S}$. The same analysis holds for the vector potential in Eq. (42). We have thus developed a mathematical method leading to general analytical solutions for the phonon polariton in semiconductor nanostructures considering the phonon dispersion and coupling between the longitudinal and transverse parts of the mechanical and electromagnetic fields. In this way we determine sets of $\mathbf{u}$, $\mathbf{A}$, and $\phi$ for each homogeneous segment of the structure, i.e., six-vector fields describing the oscillation modes of that segment. The rest of the mathematical treatment is standard: the general solution is found by superposition of these modes with arbitrary coefficients which are then determined by imposing the matching boundary conditions at the interfaces of the structure. In this manner, we also obtain the phonon-polariton dispersion relations.

## III. DOUBLE HETEROSTRUCTURES

Let us consider a DHS grown along the $z$ axis with interfaces at $z=\pm d/2$. The appropriate solutions for $\phi_h$, $\Psi$, $\nabla\times\mathbf{\Gamma}$, and $\nabla\times\mathbf{S}$ are given in Appendix A. Combining Eq. (41) and Eqs. (A7)–(A11) the vector displacement $\mathbf{u}$ is given by

$$\begin{aligned}u_x=&\{iG_1(C_3\sin k_Tz+C_4\cos k_Tz)\\&+G_2(\tilde{C}_3\sin kz+\tilde{C}_4\cos kz)\}e^{i\kappa y},\\ u_y=&\{ik_TG_1(C_1\cos k_Tz-C_2\sin k_Tz)+kG_2(\tilde{C}_1\cos kz\\&-\tilde{C}_2\sin kz)+i\kappa(C_6\sin k_Lz+\tilde{C}_6\cos k_Lz)\}e^{i\kappa y},\\ u_z=&\{\kappa G_1(C_1\sin k_Tz+C_2\cos k_Tz)-i\kappa G_2(\tilde{C}_1\sin kz\\&+\tilde{C}_2\cos kz)+k_L(C_6\cos k_Lz-\tilde{C}_6\sin k_Lz)\}e^{i\kappa y}.\end{aligned} \tag{43}$$

In the same way expressions for the vector potential **A** and the scalar potential $\phi$ are determined as follows:

$$A_x=[G_3(C_3\sin k_Tz+C_4\cos k_Tz)+iG_4(\widetilde{C}_3\sin kz+\widetilde{C}_4\cos kz)]e^{i\kappa y},$$

$$A_y=\left[k_TG_3(C_1\cos k_Tz-C_2\sin k_Tz)+ikG_4(\widetilde{C}_1\cos kz-\widetilde{C}_2\sin kz)-\kappa G_5(C_6\ \sin k_Lz+\widetilde{C}_6\cos k_Lz)+\frac{c\kappa}{\omega}(C_5\sin k_0z+\widetilde{C}_5\cos k_0z)\right]e^{i\kappa y},$$

$$A_z=\left[-i\kappa G_3(C_1\sin k_Tz+C_2\cos k_Tz)+\kappa G_4(\widetilde{C}_1\sin kz+\widetilde{C}_2\cos kz)+ik_LG_5(C_6\cos k_Lz-\widetilde{C}_6\sin k_Lz)-\frac{ic}{\omega}k_0(C_5\cos k_0z-\widetilde{C}_5\sin k_0z)\right]e^{i\kappa y}, \tag{44}$$

$$\phi=[C_5\sin k_0z+\widetilde{C}_5\cos k_0z+G_6(C_6\sin k_Lz+\widetilde{C}_6\cos k_Lz)]e^{i\kappa y}. \tag{45}$$

The coefficients $G_i$ $(i=1,\ldots,6)$ in Eqs. (43)–(45) are defined in Appendix B. An analysis of Eqs. (43) and (44) shows that the components $u_x$ and $A_x$ display independent constants and thus they are completely decoupled from the other components along the $y$ and $z$ directions. These modes are a combination of the TO phonons and a transverse electromagnetic field $A_x$ not involving the scalar potential $\phi$. This kind of mode corresponds to transverse-electric (TE) waves, the electric field being parallel to the interface: $\mathbf{E}=(E_x,0,0)$ and $\mathbf{H}=(0,H_y,H_z)$. The TE solutions can be interpreted as linear combinations of the following four linearly independent seven-vectors:

$$\begin{bmatrix} iG_1\\0\\0\\G_3\\0\\0\\0\end{bmatrix}\sin k_Tz,\quad \begin{bmatrix} iG_1\\0\\0\\G_3\\0\\0\\0\end{bmatrix}\cos k_Tz,$$

$$\begin{bmatrix} G_2\\0\\0\\iG_4\\0\\0\\0\end{bmatrix}\sin kz,\quad \begin{bmatrix} G_2\\0\\0\\iG_4\\0\\0\\0\end{bmatrix}\cos kz. \tag{46}$$

The other solutions, given by Eqs. (43)–(45), correspond to the coupled modes, which can be interpreted as transverse-magnetic (TM) waves with the electric field **E** lying in the $yz$ plane and the magnetic field **H** along the $x$ direction: $\mathbf{E}=(0,E_y,E_z)$ and $\mathbf{H}=(H_x,0,0)$. The $u_y$ and $u_z$ are combinations of transverse-TO $(k_T)$, longitudinal-LO $(k_L)$, and transverse electromagnetic parts $(k)$, while the functions $A_y$,$A_z$ have transverse and longitudinal mechanical and electromagnetic contributions. The scalar potential $\phi$ involves just longitudinal contributions ($k_L$ and $k_0$). From Eq. (19) follows that $u_y$, $A_y$, and $\phi$ have the same parity with respect to the reflection $z\rightarrow -z$; on the other hand $u_z$ and $A_z$ display the same parity between them but opposite to the other functions. From the Lorentz gauge [Eq. (2)] it is evident that the $y$ and $z$ components of **A** must have different parity. Hence, the linearly independent solutions for the TM waves are split into two groups described by the following seven-vectors:

$$\begin{bmatrix} 0\\ ik_TG_1\cos k_Tz\\ \kappa G_1\sin k_Tz\\ 0\\ k_TG_3\cos k_Tz\\ -i\kappa G_3\sin k_Tz\\ 0\end{bmatrix},\quad \begin{bmatrix} 0\\ kG_2\cos kz\\ -i\kappa G_2\sin kz\\ 0\\ ikG_4\cos kz\\ \kappa G_4\sin kz\\ 0\end{bmatrix},$$

$$\begin{bmatrix} 0\\ i\kappa\cos k_Lz\\ -k_L\sin k_Lz\\ 0\\ -\kappa G_5\cos k_Lz\\ -ik_LG_5\sin k_Lz\\ G_6\cos k_Lz\end{bmatrix},\quad \begin{bmatrix} 0\\0\\0\\0\\ (c\kappa/\omega)\cos k_0z\\ i(ck_0/\omega)\sin k_0z\\ \cos k_0z\end{bmatrix} \tag{47}$$

and

$$\begin{bmatrix} 0\\ ik_TG_1\sin k_Tz\\ -\kappa G_1\cos k_Tz\\ 0\\ k_TG_3\sin k_Tz\\ i\kappa G_3\cos k_Tz\\ 0\end{bmatrix},\quad \begin{bmatrix} 0\\ kG_2\sin kz\\ i\kappa G_2\cos kz\\ 0\\ ikG_4\sin kz\\ -\kappa G_4\cos kz\\ 0\end{bmatrix},$$

$$\begin{bmatrix} 0\\ i\kappa\sin k_Lz\\ k_L\cos k_Lz\\ 0\\ -\kappa G_5\sin k_Lz\\ ik_LG_5\cos k_Lz\\ G_6\sin k_Lz\end{bmatrix},\quad \begin{bmatrix} 0\\0\\0\\0\\ (c\kappa/\omega)\sin k_0z\\ -i(ck_0/\omega)\cos k_0z\\ \sin k_0z\end{bmatrix}. \tag{48}$$

Solution (47) corresponds to $u_y$-even, $u_z$-odd, $A_y$-even, $A_z$-odd, and $\phi$-even; solution (48) corresponds to $u_y$-odd, $u_z$-even, $A_y$-odd, $A_z$-even, and $\phi$-odd. The seven-vectors (46), (47), and (48) are each a basis for the functional subspaces of the solution space of the present problem. Such subspaces do not mix among them and should be handled separately. They provide a rather useful way for the construction of the general solutions in the case of a DHS.

Let us now consider a DHS involving the GaAs/AlAs components where the large frequency gap between the optical-phonon branches of the constituent materials permits us to apply more restrictive matching-boundary conditions of the form

(i) continuity of $\phi$, $\mathbf{A}$, and $H_T$ at the interfaces,
(ii) $\mathbf{u}=0$ at the interfaces,
(iii) continuity of $\epsilon_\infty[(\partial\phi/\partial z)-(i\omega/c)A_z]$ at the interfaces.

(49)

The conditions (49) give a rather accurate description of the polar-optical-phonon modes when retardation effects are neglected.[14,16] In this case the stress boundary conditions ($\sigma_N$ continuous at the interfaces) become unnecessary.

The solutions (46)–(48) are strictly valid for $|z|\leqslant d/2$. In the regions $|z|\geqslant d/2$ the corresponding solutions are easily found by realizing that $\mathbf{u}\equiv 0$. We are led to two kinds of solutions: *decoupled modes or TE waves*. Here $A_y=A_z\equiv 0$ and $\phi\equiv 0$, while

$$A_x=e^{i\kappa y}\begin{cases} Ce^{iK_z(z+d/2)}+\widetilde{C}e^{-iK_z(z+d/2)}; & z<-d/2\\ \pm[Ce^{-iK_z(z-d/2)}+\widetilde{C}e^{iK_z(z-d/2)}]; & z>d/2,\end{cases} \tag{50}$$

with

$$K_z=\sqrt{\epsilon_\infty^{(1)}(\omega/c)^2-\kappa^2}, \tag{51}$$

where $\epsilon_\infty^{(1)}$ is the high-frequency dielectric constant in the $|z|\geqslant d/2$ region and $+(-)$ is a label for the even (odd) states. In what follows we consider the nonradiative regime when $\kappa>\sqrt{\epsilon_\infty^{(1)}}(\omega/c)(K_z=i\mu)$ with an exponentially decaying $A_x$ for $|z|\geqslant d/2$. Applying the matching boundary conditions (49) to linear combinations of Eqs. (46) and using Eq. (50) we are led to the following results.

(a) *Odd states:*

$$u_x=iCe^{i\kappa y}\begin{cases} 0; & |z|>d/2\\ \sin k_T z-\dfrac{\sin(k_T d/2)}{\sin(kd/2)}\sin kz; & |z|<d/2,\end{cases} \tag{52}$$

$$A_x=C\,\frac{G_3}{G_1}\,e^{i\kappa y}\begin{cases} -(1+G)\sin(k_T d/2)e^{\mu(z+d/2)}; & z<-d/2\\ \sin k_T z+G\,\dfrac{\sin(k_T d/2)}{\sin(kd/2)}\sin kz; & |z|<d/2\\ (1+G)\sin(k_T d/2)e^{-\mu(z-d/2)}; & z>d/2\end{cases} \tag{53}$$

where $G=G_1G_4/G_2G_3$ and $C$ is a normalization constant. The eigenfrequencies are given after the solution of the following dispersion relation:

$$\tan(k_T d/2)=-k_T[kG\,\cot(kd/2)+(1+G)\mu]^{-1}. \tag{54}$$

(b) *Even states:*

$$u_x=iCe^{i\kappa y}\begin{cases} 0; & |z|>d/2\\ \cos k_T z-\dfrac{\cos(k_T d/2)}{\cos(kd/2)}\cos kz; & |z|<d/2,\end{cases} \tag{55}$$

$$A_x=C\,\frac{G_3}{G_1}\,e^{i\kappa y}\begin{cases} (1+G)\cos(k_T d/2)e^{\mu(z+d/2)}; & z<-d/2\\ \cos k_T z+G\,\dfrac{\cos(k_T d/2)}{\cos(kd/2)}\cos kz; & |z|<d/2\\ (1+G)\cos(k_T d/2)e^{-\mu(z-d/2)}; & z>d/2,\end{cases} \tag{56}$$

with the dispersion relation:

$$\cot(k_T d/2)=-k_T[kG\,\tan(kd/2)-(1+G)\mu]^{-1}. \tag{57}$$

In the limit $c\rightarrow\infty$ (phonon wavelengths are small compared to the reststrahlen wavelengths of the constituent materials, i.e., no retardation) the dispersion relations (54) and (57) reduce to those for the unretarded, uncoupled transverse polar-optical phonons:[16]

$$\tan(k_T d/2)=0,\quad k_T=\frac{n\pi}{d};\quad n=\text{even}$$

and

$$\cot(k_T d/2)=0,\quad k_T=\frac{n\pi}{d};\quad n=\text{odd}, \tag{58}$$

with the frequencies

$$\omega^2=\omega_0^2-\beta_T^2(\kappa^2+k_T^2), \tag{59}$$

while $A_x=0$ and the vector displacement is reduced to

$$u_x=iC\begin{cases} \sin\dfrac{n\pi}{d}z; & n=\text{even}\\ \cos\dfrac{n\pi}{d}z; & n=\text{odd}.\end{cases} \tag{60}$$

Another important limit corresponds to the nondispersive phonons $(\beta_T\rightarrow 0)$. From Eqs. (54) and (57) it follows that

$$\frac{\widetilde{k}}{\mu}\tan(\widetilde{k}d/2)=1 \tag{61}$$

and

$$\frac{\widetilde{k}}{\mu}\cot(\widetilde{k}d/2)=-1. \tag{62}$$

This case is equivalent to the results obtained by the direct solution of Maxwell's equations for the electromagnetic fields and are in complete coincidence with the dispersion relations for a semiconductor slab found by Kliewer and Fuchs in the absence of mechanical dispersion [see Eqs. (2.70) and (2.71) of Ref. 2] with

$$\widetilde{k}=\sqrt{\epsilon(\omega)(\omega/c)^2-\kappa^2},\quad \epsilon(\omega)=\epsilon_\infty\left(\frac{\omega^2-\omega_L^2}{\omega^2-\omega_0^2}\right). \tag{63}$$

Note that in this case the mechanical boundary conditions cannot be fulfilled. As can be easily seen from Eq. (46) the

TE waves give no contribution to the electric-potential-induced (Fröhlich) electron-phonon interaction. The TE waves do not have solutions in the reststrahlen region ($\omega_0 < \omega < \omega_L$) where $\epsilon(\omega) < 0$. In order to get a real $\mathbf{k}$ out of the reststrahlen region [where $\epsilon(\omega) > 0$], we should require $\kappa < (\omega/c)\sqrt{\epsilon(\omega)}$. This determines the region where Eqs. (61) and (62) have solutions.

*Coupled modes or TM waves.* In the region with $|z| > d/2$ the corresponding solutions are given by $\mathbf{u} = \mathbf{0}$, $A_x = 0$, and

$$A_y = e^{i\kappa y}\begin{cases} -\dfrac{K_z}{\kappa}\,(De^{iK_z(z+d/2)} - \widetilde{D}e^{-iK_z(z+d/2)}) + \dfrac{c\kappa}{\omega}\,(Be^{ik_z(z+d/2)} + \widetilde{B}e^{-ik_z(z+d/2)}); & z < -d/2 \\ \mp\dfrac{K_z}{\kappa}\,(De^{-iK_z(z-d/2)} - \widetilde{D}e^{iK_z(z-d/2)}) \pm \dfrac{c\kappa}{\omega}\,(Be^{-ik_z(z-d/2)} + \widetilde{B}e^{ik_z(z+d/2)}); & z > d/2, \end{cases} \tag{64}$$

$$A_z = e^{i\kappa y}\begin{cases} \pm(De^{iK_z(z+d/2)} + \widetilde{D}e^{-iK_z(z+d/2)}) + \dfrac{ck_z}{\omega}\,(Be^{ik_z(z+d/2)} - \widetilde{B}e^{-ik_z(z+d/2)}); & z < -d/2 \\ \mp(De^{-iK_z(z-d/2)} + \widetilde{D}e^{iK_z(z-d/2)}) \mp \dfrac{ck_z}{\omega}\,(Be^{-ik_z(z-d/2)} - \widetilde{B}e^{ik_z(z-d/2)}); & z > d/2, \end{cases} \tag{65}$$

$$\phi = e^{i\kappa y}\begin{cases} Be^{ik_z(z+d/2)} + \widetilde{B}e^{-ik_z(z+d/2)}; & z < -d/2 \\ \pm(Be^{-ik_z(z-d/2)} + \widetilde{B}e^{ik_z(z-d/2)}); & z > d/2. \end{cases} \tag{66}$$

In Eqs. (64)–(66) wherever a $\pm$ or $\mp$ appears the upper (lower) sign corresponds to the even (odd) potential states,

$$k_z = \sqrt{(\omega/c)^2 - \kappa^2} \tag{67}$$

and $B, \widetilde{B}, D, \widetilde{D}$ are constants.

In the nonradiative regime $k_z = i\gamma = i\sqrt{\kappa^2 - (\omega/c)^2}$ and, in order that the fields remain finite as $|z| \to \infty$, we should require $\widetilde{D} = \widetilde{B} = 0$. Applying the matching boundary conditions (49) to a linear combination of the linearly independent solutions described in Eq. (47) ($u_y$-even, $u_z$-odd, $A_y$-even, $A_z$-odd, $\phi$-even) or Eq. (48) ($u_y$-odd, $u_z$-even, $A_y$-odd, $A_z$-even, $\phi$-odd) together with Eqs. (64)–(66), we obtain for the coupled TM waves:

(a) *Even potential states:*

$$u_y = i\widetilde{C}_0 e^{i\kappa y}\begin{cases} 0; & |z| > d/2 \\ -k_T\widetilde{\Gamma}\,\cos k_T z + k\,\cos kz + \kappa\widetilde{\Gamma}_1 \cos k_L z; & |z| < d/2, \end{cases} \tag{68}$$

$$u_z = \widetilde{C}_0 e^{i\kappa y}\begin{cases} 0; & |z| > d/2 \\ -\kappa\widetilde{\Gamma}\,\sin k_T z + \kappa\,\sin kz - k_L\widetilde{\Gamma}_1 \sin k_L z; & |z| < d/2, \end{cases} \tag{69}$$

$$A_y = \frac{G_4}{G_2}\,\widetilde{C}_0 e^{i\kappa y}\begin{cases} -\widetilde{H}_1 e^{\mu(z+d/2)} + \kappa\widetilde{H}_2 e^{\gamma(z+d/2)}; & z < -d/2 \\ -\dfrac{k_T}{G}\,\widetilde{G}\,\cos k_T z - k\,\cos kz - \kappa\widetilde{\Gamma}_1(G_5 G_2/G_4)\cos k_L z - [\kappa/\cos(k_0 d/2)]\widetilde{H}_3 \cos k_0 z; & |z| < d/2 \\ -\widetilde{H}_1 e^{-\mu(z-d/2)} + \kappa\widetilde{H}_2 e^{-\gamma(z-d/2)}; & z > d/2, \end{cases} \tag{70}$$

$$A_z = \frac{iG_4}{G_2}\,\widetilde{C}_0 e^{i\kappa y}\begin{cases} \dfrac{\kappa}{\mu}\,\widetilde{H}_1 e^{\mu(z+d/2)} - \gamma\widetilde{H}_2 e^{\gamma(z+d/2)}; & z < -d/2 \\ \dfrac{\kappa}{G}\,\widetilde{\Gamma}\,\sin k_T z + \kappa\,\sin kz - k_L(G_5 G_2/G_4)\widetilde{\Gamma}_1 \sin k_L z + [k_0/\cos(k_0 d/2)]\widetilde{H}_3 \sin k_0 z; & |z| < d/2 \\ -\dfrac{\kappa}{\mu}\,\widetilde{H}_1 e^{-\mu(z-d/2)} + \gamma\widetilde{H}_2 e^{-\gamma(z-d/2)}; & z > d/2, \end{cases} \tag{71}$$

$$\phi=\frac{G_4}{G_2}\,\widetilde{C}_0 e^{i\kappa y}\begin{cases}\frac{\omega}{c}\,\widetilde{H}_2 e^{\gamma(z+d/2)}; & z<-d/2\\ G_6\,\frac{G_2}{G_4}\,\widetilde{\Gamma}_1\cos k_L z-[\omega/c\,\cos(k_0 d/2)]\widetilde{H}_3\cos k_0 z; & |z|<d/2\\ \frac{\omega}{c}\,\widetilde{H}_2 e^{-\gamma(z-d/2)}; & z>d/2\end{cases}\tag{72}$$

where $\widetilde{C}_0$ is a normalization constant. The corresponding dispersion relation is given by

$$\left[\mu\,\frac{\epsilon_\infty}{\epsilon_\infty^{(1)}}\,\sin(k_T d/2)+k_T\cos(k_T d/2)\right]\frac{\widetilde{\Gamma}}{G}+\left[\kappa\,\cos(k_L d/2)-\frac{k_L\mu}{\kappa}\,\frac{\epsilon_\infty}{\epsilon_\infty^{(1)}}\,\sin(k_L d/2)\right]\frac{4\pi\alpha c\widetilde{\Gamma}_1 G_2}{\epsilon_\infty\omega G_4}+\mu\,\frac{\epsilon_\infty}{\epsilon_\infty^{(1)}}\,\sin(kd/2)+k\,\cos(kd/2)=0.\tag{73}$$

(b) *Odd potential states:*

$$u_y=iC_0 e^{i\kappa y}\begin{cases}0; & |z|>d/2\\ -k_T\Gamma\,\sin k_T z+k\,\sin kz+\kappa\Gamma_1\sin k_L z; & |z|<d/2,\end{cases}\tag{74}$$

$$u_z=C_0 e^{i\kappa y}\begin{cases}0; & |z|>d/2\\ \kappa\Gamma\,\cos k_T z-\kappa\,\cos kz+k_L\Gamma_1\cos k_L z; & |z|<d/2,\end{cases}\tag{75}$$

$$A_y=\frac{G_4 C_0}{G_2}\,e^{i\kappa y}\begin{cases}H_1 e^{\mu(z+d/2)}-\kappa H_2 e^{\gamma(z+d/2)}; & z<-d/2\\ -\frac{k_T\Gamma}{G}\,\sin k_T z-k\,\sin kz-\kappa(G_5G_2/G_4)\Gamma_1\sin k_L z-[\kappa/\sin(k_0 d/2)]H_3\sin k_0 z; & |z|<d/2\\ -H_1 e^{-\mu(z-d/2)}+\kappa H_2 e^{-\gamma(z-d/2)}; & z>d/2,\end{cases}\tag{76}$$

$$A_z=-i\,\frac{G_4 C_0}{G_2}\,e^{i\kappa y}\begin{cases}-\frac{\kappa}{\mu}\,H_1 e^{\mu(z+d/2)}+\gamma H_2 e^{\gamma(z+d2)}; & z<-d/2\\ -\frac{\kappa\Gamma}{G}\cos\,k_T z-\kappa\,\cos kz-k_L(G_5G_2/G_4)\Gamma_1\cos k_L z-[k_0/\sin(k_0 d/2)]H_3\cos k_0 z; & |z|<d/2\\ -\frac{\kappa}{\mu}\,H_1 e^{-\mu(z-d/2)}+\gamma\kappa H_2 e^{-\gamma(z-d/2)}; & z>d/2,\end{cases}\tag{77}$$

$$\phi=\frac{G_4 C_0}{G_2}\,e^{i\kappa y}\begin{cases}-\frac{\omega}{c}\,H_2 e^{\gamma(z+d/2)}; & z<-d/2\\ (G_6G_2/G_4)\Gamma_1\sin k_L z-[\omega/c\,\sin(k_0 d/2)]H_3\sin k_0 z; & |z|<d/2\\ \frac{\omega}{c}\,H_2 e^{-\gamma(z-d/2)}; & z>d/2.\end{cases}\tag{78}$$

For the latter states the following dispersion relation is found:

$$\left[k_T\sin(k_T d/2)-\frac{\epsilon_\infty\mu}{\epsilon_\infty^{(1)}}\,\cos(k_T d/2)\right]\frac{\Gamma}{G}+\left[\kappa\,\sin(k_L d/2)+\frac{\mu k_L}{\kappa}\,\frac{\epsilon_\infty}{\epsilon_\infty^{(1)}}\,\cos(k_L d/2)\right]\frac{4\pi\alpha c}{\epsilon_\infty\omega}\,\frac{G_2\Gamma_1}{G_4}+k\,\sin(kd/2)-\frac{\epsilon_\infty}{\epsilon_\infty^{(1)}}\,\mu\,\cos(kd/2)=0.\tag{79}$$

The functions $\Gamma$, $\Gamma_1$, $\widetilde{\Gamma}$, $\widetilde{\Gamma}_1$, $H_i$, and $\widetilde{H}_i$ $(i=1,2,3)$ are given in Appendix B.

Taking the unretarded limit $(c\to\infty)$ in Eqs. (73) and (79) (and also assuming $\epsilon_\infty=\epsilon_\infty^{(1)}$) it follows that

$$\frac{(\omega_L^2-\omega^2)}{[\kappa\,\sin(k_T d/2)+k_T\cos(k_T d/2)]}\,[k_T\,\cos(k_T d/2)\sinh(\kappa d/2)-\kappa\,\sin(k_T d/2)\cosh(\kappa d/2)]=\frac{(\omega_0^2-\omega^2)}{[\kappa\,\cos(k_L d/2)-k_L\sin(k_L d/2)]}\times[k_L\sin(k_L d/2)\cosh(\kappa d/2)+\kappa\,\cos(k_L d/2)\sinh(\kappa d/2)]\tag{80}$$

for the even potential states and

$$\frac{(\omega_L^2-\omega^2)}{[\kappa\,\cos(k_T d/2)-k_T\,\sin(k_T d/2)]}\,[k_T\sin(k_T d/2)\cosh(\kappa d/2)+\kappa\,\cos(k_T d/2)\sinh(\kappa d/2)]=\frac{(\omega_0^2-\omega^2)}{[k_L\cos(k_L d/2)+\kappa\,\sin(k_L d/2)]}\times[k_L\cos(k_L d/2)\sinh(\kappa d/2)-\kappa\,\sin(k_L d/2)\cosh(\kappa d/2)] \qquad (81)$$

for the odd potential states. The above expressions correspond to the dispersion laws of the polar optical phonons in GaAs-based DHS which were reported in Ref. 16.

Another important limit is the nondispersive case ($\beta_L$, $\beta_T \to 0$). The mode frequencies can then be directly derived by solving Maxwell equations. From Eq. (73) and noting that

$$\lim\left[\mu\,\frac{\epsilon_\infty}{\epsilon_\infty^{(1)}}\,\sin(k_T d/2)+k_T\cos(k_T d/2)\right]\frac{\tilde{\Gamma}}{G}=0,$$

and

$$\lim\left[\kappa^2\cos(k_L d/2)-\frac{\epsilon_\infty}{\epsilon_\infty^{(1)}}\,k_L\mu\,\sin(k_L d/2)\right]\frac{4\pi\alpha c\tilde{\Gamma}_1}{\epsilon_\infty\omega}\,\frac{G_2}{G_4}=-\frac{\omega_L^2-\omega_0^2}{\omega^2-\omega_0^2}\,\frac{\epsilon_\infty\mu}{\epsilon_\infty^{(1)}}\sin(\tilde{k}d/2)\quad \text{for}\ \ \beta_T,\beta_L\to 0,$$

it immediately follows that

$$\frac{\tilde{k}}{\mu}\cot(\tilde{k}d/2)=-\frac{\epsilon(\omega)}{\epsilon_\infty^{(1)}}. \qquad (82)$$

In the same way, from Eq. (79) we obtain

$$\frac{\tilde{k}}{\mu}\tan(\tilde{k}d/2)=\frac{\epsilon(\omega)}{\epsilon_\infty^{(1)}}. \qquad (83)$$

The quantity $\tilde{k}$ was defined in Eq. (63). In the case of Eqs. (82) and (83) they are defined for $\omega_0<\omega<\omega_L$, where $\tilde{k}=i\tilde{\alpha}$ and $\tilde{a}=[|\epsilon(\omega)|(\omega/c)^2+\kappa^2]^{1/2}$, $\tilde{\alpha}$ being a real quantity. We are thus led to the so-called electrostatic interface modes. Such interface modes can be directly derived by applying the dielectric continuum model and correspond to Eqs. (2.44) and (2.46) of Ref. 2. Our Eqs. (73) and (79) introduce slight modifications into these interface modes in the case when $\beta_T$, $\beta_L\neq 0$. For the TM waves we also have modes outside the restsrahlen region (i.e., for $\omega<\omega_0$ and $\omega>\omega_L$).

## IV. DISCUSSION OF THE OBTAINED RESULTS

We have established a general treatment for obtaining the phonon polariton modes of semiconductor nanostructures of arbitrary geometry and composition. An essential feature of our treatment is the full consideration of the coupling between the mechanical and electromagnetic parts of the problem. Most of the existing heterogeneous semiconductor systems, and especially nanostructures, can in principle be studied by this procedure. By construction, the treatment is valid for long wavelengths ($\lambda \gg a_0$, where $a_0$ is the lattice parameter). In the case of nanostructures, due to their small dimensions, this approach, based on the application of the laws of macroscopic physics, should be within its range of applicability. The model involves a consistent formulation of the matching boundary conditions taking into account both the mechanical and electromagnetic fields. A unified and relatively simple method, providing the analytical solutions of the $7\times 7$ system of coupled differential equations for semiconductor nanostructures of a different nature and geometry, has been developed. It is shown that the solutions involve, in general, a combination of longitudinal and transverse fields. The GaAs/AlAs DHS case was studied in detail and the analytical solutions for this case are presented for both the mechanical displacements and electromagnetic fields. We have shown that, in the nonradiative regime, the model gives (a) TE waves (decoupled modes described by the $u_x$ and $A_x$ components) and with frequencies below $\omega_0$ and above $\omega_L$ and with $\kappa<\sqrt{\epsilon(\omega)}(\omega/c)$, (b) TM waves involving coupled modes with a mixed LO–TO character and expressed by the $u_y$ and $u_z$ components of the mechanical displacements and the $A_y$ and $A_z$ components of the electromagnetic vector potential (in the Lorentz gauge the scalar potential $\phi$ is not independent of the above quantities and can be directly derived once the former are known). For this latter case we find interface-phonon-polariton modes in the frequency range $\omega_L<\omega<\omega_0$ and in the regions below $\omega_0$ and above $\omega_L$ other modes are also detected.

The dispersion law of the Kliewer-Fuchs model for polariton modes and the unretarded coupled modes of Refs. 16 and 18 were derived as the appropriate limiting cases of Eqs. (54), (57), (73), and (79) of the present work. It is worthwhile to analyze the relation of our treatment with that of Ref. 2. As established above, our equations contain those of Kliewer and Fuchs as a limit when $\beta_T,\beta_L\to 0$. The introduction of such parameters in our treatment bears an important methodological role allowing us to make a mathematical discussion on the basis of coupled differential equations (instead of the integral equations of Ref. 2). This permits us to introduce the complete matching boundary conditions of the problem (mechanical and electromagnetic) providing a fully consistent treatment of the normal modes. Our approach is flexible and allows the analysis of different geometries of the possible nanostructures. In the DHS case the influence of the corrections related to the $\beta$'s (for values typically of the order of $10^5$ cm/seg) is of importance just for the lower values of $d$ ($d\sim 1-10$ nm). For larger values of $d$ the relative influence of these corrections is negligible and we are essentially led to the results of Kliewer and Fuchs.

In Fig. 1 we show for the TE (odd) modes the dependence of the frequency $\omega$ on in-plane wave vector $\kappa$ for different modes (dispersion relations) in the region $\omega<\omega_0$ and taking $d=3$ nm. For the numerical calculations the parameters of GaAs and AlAs of Ref. 16 were used. As corresponds to the nonradiative regime, the curves are at the right-hand side of the straight line $\omega=c(\epsilon_\infty^{(1)})^{-1/2}\kappa$. They emerge from that line and bear a weak electromagnetic component, resembling the uncoupled TO polar-optical phonons.[16] It can be seen, as expected, that the curves do not show significant dispersion (they are very flat). Hence, in this region we are essentially

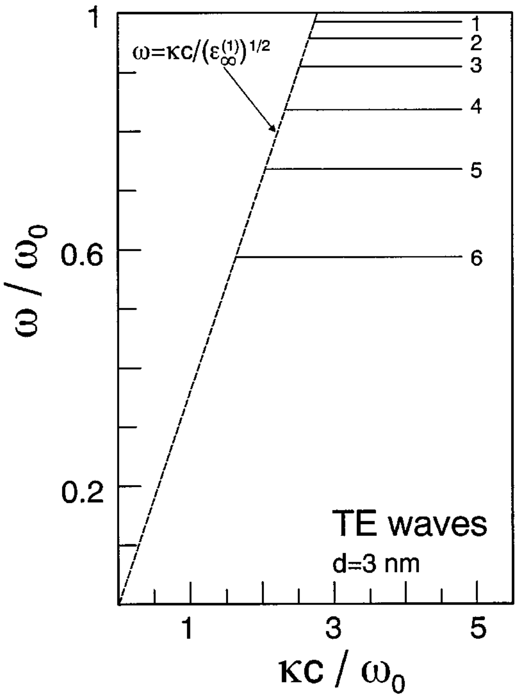


FIG. 1. Dispersion relation of the decoupled TE modes in a 3-nm-wide GaAs/AlAs DHS for the odd states [Eq. (54)] in the region $\omega<\omega_0$. For the numerical calculations the values of parameters of Ref. 16 were used. The photon dispersion relation $\omega=\kappa c/(\epsilon_\infty^{(1)})^{1/2}$ for the AlAs is shown as a dashed line.

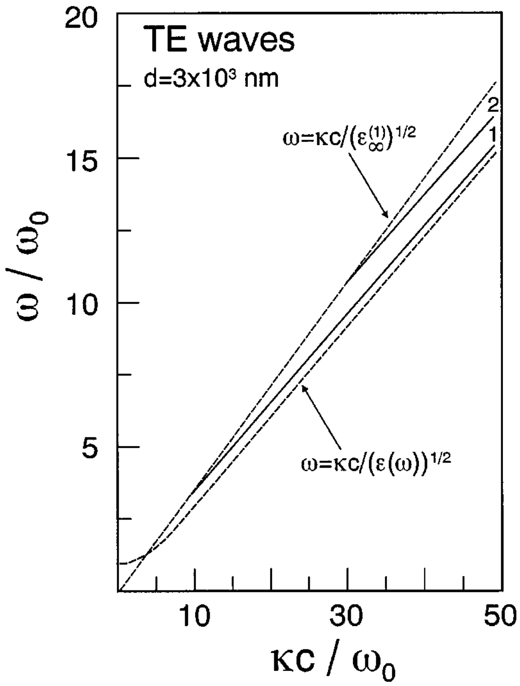


FIG. 2. As Fig. 1 for a $3\times10^3$ nm wide DHS and $\omega>\omega_L$. The photon-dispersion relation $\omega=\kappa c/(\epsilon(\omega))^{1/2}$ in the frequency region of the GaAs optical phonon and $\omega=\kappa c/(\epsilon_\infty^{(1)})^{1/2}$ are shown as dashed lines.

led to the $\kappa\rightarrow0$ limit of the phonon dispersion curves for the uncoupled modes.[16] In the frequency interval $\omega_0<\omega<\omega_L$ we do not have TE modes, as expected from general principles. For $\omega>\omega_L$ we obtain high-frequency modes essentially of electromagnetic nature. We have set $d=3\times10^3$ nm in Fig. 2, a relatively large $d$ value. For much smaller values of $d$ the corresponding frequencies become too large (visible region and beyond). As in Fig. 1, the curves of Fig. 2 are at the right of the photon straight line but above the hyperbola $\omega=c(\epsilon(\omega))^{-1/2}\kappa$. These high modes exist only when retardation effects are included.[2] They begin on the line $\omega=\kappa c/(\epsilon_\infty^{(1)})^{1/2}$ and can be considered as waves mainly confined to the interior of the DHS. The small size of the heterostructure gives rise to standing waves with predominant electromagnetic character for the value of $d$ given in Fig. 2. Of course, the large values of $d$ here considered are not typical for DHS usually grown by molecular beam epitaxy. Hence, this kind of mode is not relevant for usual DHS. Let us now analyze the coupled TM modes. We again have modes in the intervals $\omega<\omega_0$ and $\omega>\omega_L$. Very interesting are, in this case, the interfacelike modes in the interval $\omega_0<\omega<\omega_L$. In Fig. 3 we show these modes for three values of $d$. These results are very similar to those of Kliewer and Fuchs. Let us recall that in the region $\epsilon(\omega)<0$ all the curves emerge from the same lower limit (crossing of the straight line for the photon with the $\omega=\omega_0$ horizontal line). This result is at variance with the corresponding result for bulk polar-optical phonons, where the high-frequency curves for the interface modes emerge from the $\omega=\omega_L$ horizontal line (at $\kappa=0$). When $\kappa\rightarrow\infty$ all the curves asymptotically approach a horizontal line corresponding to $\omega=\omega_I$ for $\epsilon(\omega_I)=-\epsilon_\infty^{(1)}$ as seen in the figure. The curves of Fig. 3 were constructed from Eqs. (82) and (83), taking $\tilde{k}=i\tilde{\alpha}$ [i.e., we are limiting ourselves to the case $\beta\rightarrow0$ of Eqs. (73) and (79)]. The corrections introduced by the $\beta$'s are relevant for the smaller $d$ values (for instance, $d\sim3$ nm); otherwise the results for interface polariton modes essentially coincide with those of Kliewer and Fuchs. It should be possible to observe the deviation between experimental data for forward scattering (which should follow the

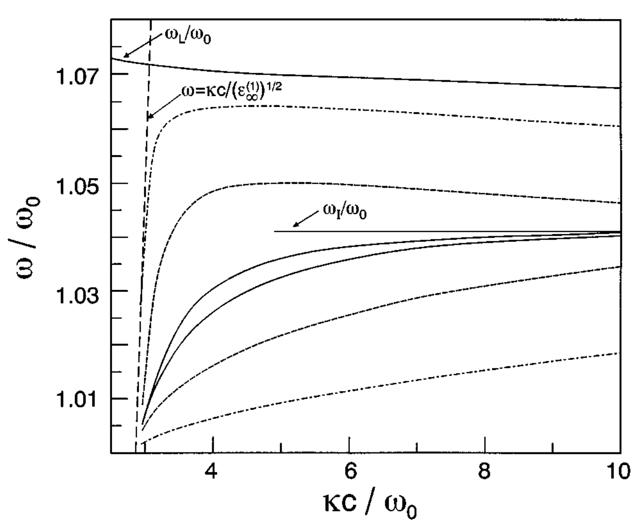


FIG. 3. Dispersion relations of interface-phonon polaritons in GaAs/AlAs DHS for $d=3\times10^3$ nm (solid lines), $d=1\times10^3$ nm (short-dashed lines), and $d=300$ nm (dot-dashed lines) calculated following Eqs. (82) and (86). The horizontal line indicates the asymptotic frequency value $\omega_I$ of the modes for $\kappa\rightarrow\infty$ given by $\epsilon(\omega_I)=-(\epsilon_\infty^{(1)})$. The unretarded interface mode for $d=300$ nm is indicated by the highest-frequency solid line.

calculations including retardation) and the theory without retardation also shown in Fig. 3.

It is also interesting to discuss the radiative modes, which should appear for frequencies at the left-hand side of the photon curve $\omega = c(\epsilon_\infty^{(1)})^{-1/2}\kappa$. In that case we no longer have vibrational eigenstates in the strict sense. The system loses energy in the form of radiation. However we can speak of certain *virtual modes* characterized by a complex frequency.[3] Radiative modes are of interest for a discussion of the optical properties in the *ir* region and require a somewhat different solution of the equations which may be discussed in future work.

## ACKNOWLEDGMENTS

One of us (C.T.G.) acknowledges the hospitality of the Max-Planck-Institut für Festkörperforschung, where part of this work was performed. We are grateful to H. Calas for his stimulating interest in this work and Andres Cantarero for a critical reading of the manuscript.

## APPENDIX A: VECTOR HELMHOLTZ EQUATION: CARTESIAN COORDINATES

For Cartesian coordinates the solution of the vector Helmholtz equation is

$$(\nabla^2 + q^2)\mathbf{F} = 0, \tag{A1}$$

with $\nabla \cdot \mathbf{F} = 0$ is given by[22]

$$\mathbf{F} = \mathbf{F}_1(x,y,z) + \mathbf{F}_2(x,y,z) + \mathbf{F}_3(x,y,z), \tag{A2}$$

where

$$\mathbf{F}_1 = \nabla \times (v\,\mathbf{e}_z); \quad \mathbf{F}_2 = \frac{1}{q}\,\nabla \times \nabla(v\,\mathbf{e}_z); \quad \mathbf{F}_3 = \nabla u. \tag{A3}$$

The functions $v(x,y,z)$ and $u(x,y,z)$ must satisfy the following equations:

$$(\nabla^2 + q^2)v = 0 \quad \text{and} \quad \nabla^2 u = 0. \tag{A4}$$

The solution $\mathbf{F}_3$ is not relevant to the present problem since we only need $\nabla \times \mathbf{F}$. The general solution of the equation for $v$, taking into account the translational symmetry in the $x,y$ plane, is of the form:

$$v(x,y,z) = (C \sin\xi z + \tilde{C} \cos\xi z)e^{i\boldsymbol{\kappa}\cdot\mathbf{R}}, \tag{A5}$$

where $\boldsymbol{\kappa} \equiv (k_x, k_y)$, $\mathbf{R} \equiv (x,y)$, $\xi^2 = q^2 - \kappa^2$, $C$, and $\tilde{C}$ are constants. Hence, the solution of (A1) is given by

$$\mathbf{F} = i(k_y\mathbf{e}_x - k_x\mathbf{e}_y)(C_1\sin\xi z + C_2\cos\xi z)e^{i\boldsymbol{\kappa}\cdot\mathbf{R}} + i\,\frac{\xi\boldsymbol{\kappa}}{q}\,(C_3\cos\xi z - C_4\sin\xi z)e^{i\boldsymbol{\kappa}\cdot\mathbf{R}} + \frac{\kappa^2}{q}\,\mathbf{e}_z(C_3\sin\xi z - C_4\cos\xi z)e^{i\boldsymbol{\kappa}\cdot\mathbf{R}}. \tag{A6}$$

Applying solutions of the type (A6) to Eq. (36), the expressions for $\boldsymbol{\Gamma}$ and $\mathbf{S}$ are obtained from Eqs. (32) and (33), respectively. The present problem shows invariance under arbitrary rotations about the $z$ axis. Taking advantage of this symmetry we choose the $y$ axis along the in-plane wave vector $\boldsymbol{\kappa}$ without loss of generality. Hence, we have $\boldsymbol{\kappa} \equiv (0,k_y)$. We now write the final expressions for $\nabla \times \boldsymbol{\Gamma}$ and $\nabla \times \mathbf{S}$:

$$\nabla \times \boldsymbol{\Gamma} = e^{i\kappa y}\Bigg\{\Bigg[i(C_3\sin k_T z + C_4\cos k_T z) + \frac{1}{a(1+b)}\,(\tilde{C}_3\sin kz + \tilde{C}_4\cos kz)\Bigg]\mathbf{e}_x + \Bigg[ik_T(C_1\cos k_T z - C_2\sin k_T z) + \frac{k}{a(1+b)}\,(\tilde{C}_1\cos kz - \tilde{C}_2\sin kz)\Bigg]\mathbf{e}_y + \Bigg[\kappa(C_1\sin k_T z + C_2\cos k_T z) - \frac{i\kappa}{a(1+b)}\,(\tilde{C}_1\sin kz + \tilde{C}_2\cos kz)\Bigg]\mathbf{e}_z\Bigg\}, \tag{A7}$$

$$\nabla \times \mathbf{S} = e^{i\kappa y}\{[i(\tilde{C}_3\sin kz + \tilde{C}_4\cos kz) - a(1-b)(C_3\sin k_T z + C_4\cos k_T z)]\mathbf{e}_x + [ik(\tilde{C}_1\cos kz - \tilde{C}_2\sin kz) - a(1-b)k_T(C_1\cos k_T z - C_2\sin k_T z)]\mathbf{e}_y + [\kappa(\tilde{C}_1\sin kz + \tilde{C}_2\cos kz) + ia(1-b)\kappa(C_1\sin k_T z + C_2\cos k_T z)]\mathbf{e}_z\}, \tag{A8}$$

where

$$k_T = \left[\frac{1}{\beta_T^2}\,(\omega_0^2 - \omega^2) - \frac{4\pi\omega^2}{c^2 a(1+b)} - \kappa^2\right]^{1/2},$$

$$k = \left[\epsilon_\infty(\omega/c)^2 - \frac{\alpha^2 a(1-b)}{\rho\beta_T^2} - \kappa^2\right]^{1/2}. \tag{A9}$$

The solutions for $\Psi$ and $\phi_h$ are

$$\Psi = (C_6\sin k_L z + \tilde{C}_6\cos k_L z)e^{i\kappa y},$$

$$\phi_h = (C_5\sin k_0 z + \tilde{C}_5\sin k_0 z)e^{i\kappa y}, \tag{A10}$$

with

$$k_L = \left[\frac{1}{\beta_L^2}\,(\omega_L^2 - \omega^2) - \kappa^2\right]^{1/2}, \quad k_0 = [(\omega/c)^2 - \kappa^2]^{1/2}. \tag{A11}$$

## APPENDIX B: VALUES OF PARAMETERS CONTAINED IN THE MAIN TEXT

The coefficients $G_i$ $(i=1,\ldots,6)$ are

$$G_1=-\frac{\beta_T^2}{\omega_0^2}+\frac{c^2a(1-b)}{4\pi\omega_0^2\omega^2}\,(\omega_L^2-\omega_0^2), \tag{B1}$$

$$G_2=-\frac{\beta_T^2}{\omega_0^2}\,\frac{1}{a(1+b)}+\frac{c^2}{4\pi\omega_0^2\omega^2}\,(\omega_L^2-\omega_0^2), \tag{B2}$$

$$G_3=\frac{\alpha c^3}{\epsilon_\infty\omega_0^2}\left[\frac{a(1-b)}{\omega^3}\,(\omega_0^2-\omega^2)+\frac{4\pi}{\omega}\,(\beta_T/c)^2\right], \tag{B3}$$

$$G_4=\frac{\alpha c^3}{\epsilon_\infty\omega_0^2}\left[\frac{1}{\omega^3}\,(\omega^2-\omega_0^2)-\frac{4\pi}{\omega a(1+b)}\,(\beta_T/c)^2\right], \tag{B4}$$

$$G_5=\frac{4\pi\alpha\beta_L^2}{\epsilon_\infty c}\,\omega\{\omega^2[1+(\beta_L/c^2)]-\omega_L^2\}^{-1}, \tag{B5}$$

and

$$G_6=\frac{(\omega^2-\omega_L^2)c}{\beta_L^2\omega}\,G_5. \tag{B6}$$

Other parameters present in the main text are

$$\tilde{\Gamma}=[kk_L\cos(kd/2)\sin(k_Ld/2)+\kappa^2\,\sin(kd/2)\cos(k_Ld/2)]\,[k_Tk_L\cos(k_Td/2)\sin(k_Ld/2)+\kappa^2\sin(k_Td/2)\cos(k_Ld/2)]^{-1}, \tag{B7}$$

$$\tilde{\Gamma}_1=\kappa[k_T\sin(kd/2)\cos(k_Td/2)-kT\sin(k_Td/2)\cos(kd/2)]\times[k_Tk_L\cos(k_Td/2)\sin(k_Ld/2)+\kappa^2\sin(k_Td/2)\cos(k_Ld/2)]^{-1}, \tag{B8}$$

$$\Gamma=[kk_L\sin(kd/2)\cos(k_Ld/2)+\kappa^2\,\cos(kd/2)\sin(k_Ld/2)]\times[k_Tk_L\sin(k_Td/2)\cos(k_Ld/2)+\kappa^2\,\cos(k_Td/2)\sin(k_Ld/2)]^{-1}, \tag{B9}$$

$$\Gamma_1=\kappa[k_T\sin(k_Td/2)\cos(kd/2)-k\,\sin(kd/2)\cos(k_Td/2)]\times[k_Tk_L\sin(k_Td/2)\cos(k_Ld/2)+\kappa^2\cos(k_Td/2)\sin(k_Ld/2)]^{-1}, \tag{B10}$$

$$\tilde{H}_1=\frac{\tilde{\Gamma}}{G}\,k_T\cos(k_Td/2)+k\,\cos(kd/2)+\frac{4\pi\alpha c\kappa}{\epsilon_\infty\omega}\,\tilde{\Gamma}_1\,\frac{G_2}{G_4}\,\cos(k_Ld/2), \tag{B11}$$

$$\tilde{H}_2=\frac{4\pi\alpha c}{\epsilon_\infty\omega}\,\frac{G_2}{G_4}\,\frac{\omega^2-\omega_L^2}{\omega^2[(\beta_L/c)^2+1]-\omega_L^2}\,\tilde{\Gamma}_1\cos(k_Ld/2)-\tilde{H}_3, \tag{B12}$$

$$\tilde{H}_3=\left\{\left(1-\frac{\epsilon_\infty}{\epsilon_\infty^{(1)}}\right)\kappa\left(\frac{\tilde{\Gamma}}{G}\,\sin(k_Td/2)+\sin(kd/2)\right)-\frac{4\pi\alpha c}{\epsilon_\infty\omega}\,\frac{G_2}{G_4}\,\tilde{\Gamma}_1\left[\frac{(\omega^2-\omega_L^2)\gamma\,\cos(k_Ld/2)}{\omega^2[(\beta_L/c)^2+1]-\omega_L^2}+\frac{(\omega\beta_L/c)^2k_L\sin(k_Ld/2)}{\omega^2[1+(\beta_L/c)^2]-\omega_L^2}-\frac{\epsilon_\infty}{\epsilon_\infty^{(1)}}\,k_L\sin(k_Ld/2)\right]\right\}[k_0\tan(k_0d/2)-\gamma]^{-1}, \tag{B13}$$

$$H_1=\frac{k_T\Gamma}{G}\,\sin(k_Td/2)+k\,\sin(kd/2)+\frac{4\pi\alpha c\kappa}{\epsilon_\infty\omega}\,\frac{G_2}{G_4}\,\Gamma_1\sin(k_Ld/2), \tag{B14}$$

$$H_2=\frac{4\pi\alpha c}{\epsilon_\infty\omega}\,\frac{G_2}{G_4}\,\Gamma_1\,\frac{\omega^2-\omega_L^2}{\omega^2[1+(\beta_L/c)^2]-\omega_L^2}\,\sin(k_Ld/2)-H_3, \tag{B15}$$

$$H_3=\left\{\left(1-\frac{\epsilon_\infty}{\epsilon_\infty^{(1)}}\right)\kappa\left(\frac{\Gamma}{G}\,\cos(k_Td/2)+\cos(kd/2)\right)+\frac{4\pi\alpha c}{\epsilon_\infty\omega}\,\frac{G_2}{G_4}\,\Gamma_1\left[\frac{(\omega^2-\omega_L^2)\gamma\,\sin(k_Ld/2)}{\omega^2[1+(\beta_L/c)^2]-\omega_L^2}-\frac{(\omega\beta_L/c)^2k_L\cos(k_Ld/2)}{\omega^2[1+(\beta_L/c)^2]-\omega_L^2}+\frac{\epsilon_\infty}{\epsilon_\infty^{(1)}}\,k_L\cos(k_Ld/2)\right]\right\}\times[k_0\cot(k_0d/2)+\gamma]^{-1}. \tag{B16}$$

*Also at Dept. of Theoretical Physics, Univ. of Havana, 10400 C, Havana, Cuba.

[1] *Light Scattering in Solids V*, edited by M. Cardona and G. Güntherodt (Springer, Heidelberg, 1989).
[2] K. L. Kliewer and R. Fuchs, Phys. Rev. **144**, 495 (1966).
[3] K. L. Kliewer and R. Fuchs, Phys. Rev. **150**, 573 (1966).
[4] R. Ruppin and R. Englman, Rep. Prog. Phys. **33**, 149 (1970).
[5] S. Ushioda and R. Loudon, in *Surface Polaritons*, edited by V. M. Agranovich and D. L. Mills (North-Holland, Amsterdam, 1982), p. 535.
[6] S. Ushioda, *Progress in Optics*, edited by E. Wolf (North-Holland, Amsterdam, 1982), Vol. 19, p. 139.
[7] M. Babiker, J. Phys. C **19**, 683 (1986), see also references therein.
[8] B. K. Ridley and M. Babiker, Phys. Rev. B **43**, 9096 (1991).
[9] W. Liu, G. Eliasson, and J. J. Quinn, Solid State Commun. **55**, 533 (1985).

[10] J. S. Nkoma, Solid State Commun. **64**, 1383 (1987).
[11] N. Raj and D. R. Tilley, Solid State Commun. **55**, 373 (1985).
[12] Ph. Lambin, J. P. Vigneron, A. A. Lucas, and A. Dereaux, Phys. Scr. **35**, 343 (1987), and references therein.
[13] A. Elangoran and K. Navaneethakrishnan, Solid State Commun. **89**, 459 (1994).
[14] M. P. Chamberlain, M. Cardona, and B. K. Ridley, Phys. Rev. B **48**, 14 356 (1993); M. P. Chamberlain and M. Cardona, Semicond. Sci. Technol. **9**, 749 (1994).
[15] B. A. Foreman, Phys. Rev. B **52**, 12 260 (1995).
[16] F. Comas, R. Pérez-Alvarez, C. Trallero-Giner, and M. Cardona, Superlattices Microstruct. **14**, 95 (1994).
[17] C. Trallero-Giner, F. García-Moliner, R. V. Velasco, and M. Cardona, Phys. Rev. B **45**, 11 944 (1992).
[18] C. Trallero-Giner and F. Comas, Philos. Mag. B **70**, 583 (1994).
[19] F. Comas and C. Trallero-Giner, Physica B **192**, 394 (1993).
[20] The equations obtained are not valid for the treatment of strong interface effects as in InAs/GaSb systems. Following the Foreman model of Ref. 15 and introducing adequate $\delta$ *functions* in the reduced mass Eq. (5) can be generalized to such systems. The matching-boundary conditions are easily derived by the same procedures as in Sec. II.
[21] M. Born and K. Huang, *Dynamical Theory of Crystal Lattices* (Clarendon, Oxford, 1988).
[22] P. M. Morse and H. Feshbach, *Methods of Theoretical Physics* (McGraw-Hill, New York, 1953).